Research Article Vol. 56, No. 23 / August 10 2017 / Applied Optics 6577

applied optics

Detection and characterization of chemical aerosol using laser-trapping single-particle Raman spectroscopy

Aimable Kalume,[1] Leonid A. Beresnev,[1] Joshua Santarpia,[2] and Yong-Le Pan[1,*]

[1]U.S. Army Research Laboratory, 2800 Powder Mill Rd, Adelphi, Maryland 20783, USA
[2]Sandia National Laboratory, Albuquerque, New Mexico 87123, USA
*Corresponding author: yongle.pan.civ@mail.mil

Received 14 April 2017; revised 10 July 2017; accepted 12 July 2017; posted 13 July 2017 (Doc. ID 292709); published 9 August 2017

Detection and characterization of the presence of chemical agent aerosols in various complex atmospheric environments is an essential defense mission. Raman spectroscopy has the ability to identify chemical molecules, but there are limited numbers of photons detectable from single airborne aerosol particles as they are flowing through a detection system. In this paper, we report on a single-particle Raman spectrometer system that can measure strong spontaneous, stimulated, and resonance Raman spectral peaks from a single laser-trapped chemical aerosol particle, such as a droplet of the VX nerve agent chemical simulant diethyl phthalate. Using this system, time-resolved Raman spectra and elastic scattered intensities were recorded to monitor the chemical properties and size variation of the trapped particle. Such a system supplies a new approach for the detection and characterization of single airborne chemical aerosol particles.

OCIS codes: (300.6450) Spectroscopy, Raman; (120.5820) Scattering measurements; (010.1100) Aerosol detection; (140.7010) Laser trapping; (120.6200) Spectrometers and spectroscopic instrumentation.

https://doi.org/10.1364/AO.56.006577

1. INTRODUCTION

Despite considerable efforts vowing to prevent the development, production, stockpiling, and the use of chemical weapons [1], the recent surge in the number of deadly attacks carried out by terrorists has increased the sense of threat and fear among the public, leading to an urgent need for more efficient methods of rapid detection and characterization of various chemical agents [2,3]. For obvious safety-related reasons, most of the preliminary experimental studies are conducted over a wide range of chemical simulant bulks, rather than handling them in aerosol format, nor highly hazardous and lethal compounds [2,3]. While these chemicals can be studied by other analytical means, our particular goal is to spectroscopically interrogate chemical agents and their simulants as aerosols. In this work, we propose and develop a novel method, and utilize it to characterize diethyl phthalate (diethyl 1,2-benzene dicarboxylate, DEPh), a safe chemical simulant of the lethal VX nerve agent [4,5]. The method is realized by recording a series of time-resolved Raman spectra and scattering intensities of a single optically trapped microdroplet, and also obtaining them from a series of single optically trapped microdroplets in air.

Since the introduction of single-particle manipulation by electrodynamic balances in 1953 [6], followed by optical levitation in the 1970's [7,8], and vibrating orifice aerosol generators (VOAG) [9] in 1973, there have been tremendous efforts in the development of aerosol science and applications [10,11]. Within the aerosol study, most of the measurements of Raman spectra were accumulated from a series of continuously flowing through microdroplets, trapped or levitated single particles, or particles deposited on a substrate. The unique property of VOAG of producing identical airborne droplets enabled Raman spectra to be captured from a series of identical particles. Optical trapping of a microparticle in air is more challenging than in liquid because of the drag force in air and the larger optical scattering force due to the higher refractive index contrast in air. As a result, there have been quite a lot of pioneering studies of Raman spectra from single airborne particles [12–22], but limited for the detection and characterization from single chemical agent aerosols.

In the past, most single-laser optical trapping techniques were only designed to trap either absorbing particles (via photophoretic forces) [19,23] or nonabsorbing particles (via radiative pressure forces) [24,25]. Our laboratory has successfully developed an efficient technique to trap either type of particles using relatively low numerical aperture (NA = 0.55) optics in the air without using a large NA > 1.0 microscopic objective, e.g., [26]. As particles can be trapped a centimeter away from any optical surface in this new technique, it greatly reduces the

possibility of contamination for optical components and can be easily integrated to a wide range of characterization techniques, scrutinizing physical properties (size, evaporation rate, refractive index, and temperature) or chemical properties (composition, photochemistry, reactivity, and ionic strength). Combination of single-particle trapping with various spectroscopic characterization methods has proven to be an invaluable tool in ascertaining crucial information about the particle. For instance, depending on the vibrations within a molecule, Raman spectroscopy provides a substantial insight on the chemical composition of the particle as well as studies on phase and size transitions, liquid-gas interactions, thermodynamic behavior, and the kinetics of mass transfer in airborne droplets [12–18].

For more than a century, the Lorenz–Mie theory (LMT) [27,28] has been at the core of interpreting light scattering from dielectric spherical particles and associated properties [29,30]. LMT predicts sharp rises (resonances) in elastically scattered intensity when measured as a function of particle size or scattering angle. Recent studies improved on the classical LMT and expanded it from its initially simple and uniform concept to other scenarios, including various beam shapes and particles with unique properties [31]. By comparison of the scattered intensity at a certain angle, measured as function of time, with the computed resonance structure, one can precisely determine the size of the trapped spherical particles at any given time.

In this study, we report the capture of individual diethyl phthalate and glycerol microdroplets by single-laser trapping in air, followed by Raman spectroscopic characterization. To the best of our knowledge, this is the first observation of Raman spectra from diethyl phthalate in single-droplet format. In addition to the spontaneous Raman peaks reported in bulk liquid [32,33], the microdroplet Raman spectrum exhibits additional features: stimulated Raman scattering (SRS) and morphology-dependent resonances also known as whispering-gallery-modes (WGMs) [16,34]. These additional signature peaks enhance the uniqueness of characterizing a chemical fingerprint of the single microdroplet being studied [34–36]. Based on our advanced trapping technique, which can trap large particles (a few tens of micrometers versus a few micrometers) at long working distance (a centimeter versus a few micrometers) with high trapping efficiency (captures one from a few particles versus from hundreds), this newly developed laser-trapping, single-particle, Raman spectroscopic technology reported here demonstrates the potential in determining the chemical composition and particle size of airborne chemical aerosol particles.

2. EXPERIMENTAL AND THEORETICAL METHODS

A schematic of the experimental setup used in this study is shown in Fig. 1. A liquid sample of diethyl phthalate or glycerol (Sigma Aldrich, 99.5% stated purity), held in a 25 mL glass bottle, was used without further purification. Microdroplets (typical size: 20–25 μm) were generated using a low-temperature drop-on-demand single-jet piezoelectric dispensing device (Microfab MJ-ATP-01, 30 μm diameter orifice), actuated by a Microfab power supply (JetDrive III controller). Computer software (JetServer4) allowed the adjustment of jetting conditions by

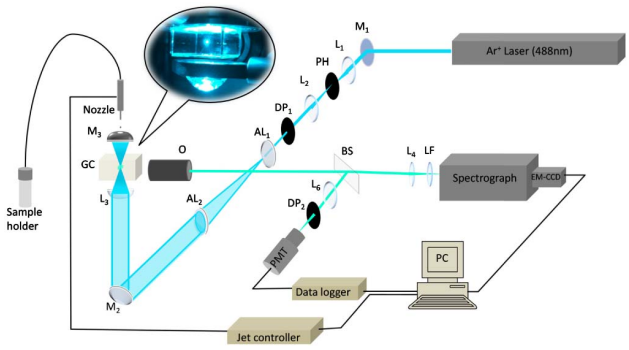

Fig. 1. Schematic of the experimental setup for a laser-trapping single-particle Raman spectroscopic system. **M_i**: mirror, **L_i**: lens, **PH**: pin hole, **DP_i**: diaphragm, **AL_i**: axicon lens, **O**: objective lens, **GC**: glass cell, **BS**: beam splitter, **LF**: long-pass filter, **EM-CCD**: electron multiplying charge coupled device, **PMT**: photomultiplier tube.

varying the repetition rate, applied voltage, and time delays. The jetting nozzle was mounted on a 3D linear translational stage to enable spatial adjustment during the experiments.

In order to improve the trapping efficiency and robustness, the trapping system was modified into a confocal hollow trapping scheme similar to the setup described in our previous articles [26,37,38]. They reported the detail mechanism and force calculation [26] of this new trap design, demonstrated how to deliver particle to the trapping volume [37], and compared various trapping configurations [38]. A single laser beam from a continuous wave (CW) Ar-ion laser operating at 488 nm with an output power ~750 mW, was used. The original Gaussian beam was converted into a hollow beam, with a ring-shaped transverse cross section by passing through two axicon lenses (Del Mar Photonics, cone angle 175°). The horizontally propagating hollow beam was reflected to the vertical by an elliptical mirror set at 45°, propagated through an aspheric lens (with NA = 0.55), and focused onto a point centered inside a containment glass cell (25 mm × 25 mm× 15 mm). Beyond the focal point, the conical beam expanded up onto a concave spherical mirror (f = 19 mm, diameter = 25.4 mm), reflected back to overlap with the upward-propagating beam cone, and refocused at a second focal point aligned with the same beam axis. The concave mirror was mounted on a 2D tiltable 3D linear translational stage, and the second focal point could be independently shifted, in 3D, inside the cell. Ideal conditions would occur when the two focal points were perfectly aligned with each other with a few tens of microns separation vertically. Note that, two holes ($\phi \sim 8$ mm), at the center of the concave mirror and the glass cell, allow microdroplets ejected from the nozzle to reach the trapping area. The same trapping laser was also used as the excitation source for Raman scattering. Scattered light from the single trapped particle was collected with a microscopic objective lens (Mitutoyo, M Plan Apo HL, NA = 0.42), and focused by a second lens prior to entering the spectrograph (Princeton Instruments Isoplane SCT320) through a narrow slit. A long-pass filter at the entrance of the spectrograph served to block the elastically scattered 488 nm laser light. A 1200 lines/mm grooved grating with a blaze wavelength at

750 nm was used to disperse the Raman scattered light, and the spectra were recorded by an electron-multiplying charge-coupled device (EMCCD, Princeton Instruments, ProEM) camera. Spectra were continuously recorded over a 1 or 2 min interval with a 2 s. accumulation window. Data were processed on a lab computer using the Princeton Instruments LightField software.

As shown in Fig. 1, a portion of the collected scattered light was reflected by a dichroic beam splitter (cutoff wavelength 488.5 nm) and directed toward a photomultiplier tube (PMT), to monitor the total intensity variation of the 488 nm elastically scattered light at 90° (±2°) with respect to the incident beam propagation direction, during the spectral recording period. The PMT signal was digitized with a data logger (DATAQ DI-2018 series) prior to being recorded and processed with WinDaq software. In addition, a simulated resonance spectrum was computed according to the Lorenz–Mie theory.

3. RESULTS AND DISCUSSION

Our experimental results showed relatively high efficiency and reproducibility in microdroplet generation and trapping. First, the trapping laser was optimized, with the uniform ring-shaped beams tightly focused and overlapping at the center of the glass cell. The jetting conditions were adjusted to match the available trapping forces at the focal point by manipulating the velocity, size, orientation, and trajectory of the microdroplets. In contrast to the classical approach relying on high concentration of particles [39], our system was generating droplets (typical initial diameter of 20–25 μm, $4.1 \sim 8.2 \times 10^{-12}$ L in volume) at a 1 Hz repetition rate and we were able to easily trap one in five generated particles. This approach could be very useful when working with hazardous material or in situations where sample quantities are limited from complex atmospheric environments. It supplies the potential for detection and characterization chemical aerosols continuously sampled from the atmosphere.

As shown in Fig. 2 and Table 1, in addition to the peaks resulting from spontaneous Raman scattering observed from bulk liquid, strong transitions due to stimulated Raman scattering (SRS) process were observed at $\Delta\upsilon = 231$, 363, 387, 540, 568, 588, and 1054 cm^{-1} only from the droplets. Our study shows a typical example of internally seeded SRS, where spontaneous Stokes photons injected into the medium lead to the amplification of the Raman transitions by total internal reflection within the droplet. While a spontaneous Raman signal is generally weak and requires special care in optical design, stimulated Raman exhibits stronger and sharper profiles compared to bulk liquid peaks (up to ~25 times in our experiments). Fully exploited, this phenomenon can be useful to study small frequency differences or to detect minority species in complex environments [40,41]. Note that relative intensities of stimulated Raman scattering depend on the angle of observation. In our experiments, the collecting lens was set at 90° with respect to the excitation laser, and in this configuration the scattered light results from a more uniform spatial distribution within the microdroplet [11]. As demonstrated by Chak and co-workers, Raman intensities from different areas of a droplet can be spatially resolved using the image reserved spectrograph and a 2D detector [42]. However, the spectra reported in this work were accumulated across a large solid angle (NA = 0.42) and vertically binned in the 2D EMCCD, so we did not consider the possible differences of Raman spectra from different angles and areas of the droplet.

Previous works [43–45] have reported the observation of "whispering-gallery-modes" (WGMs) of fluorescence and Raman scattering resonance in a microcavity due to the radiation waves propagating at the concave interface of the

Table 1. Raman Shift Frequencies of Diethyl Phthalate, in Comparison with Results from Previous Works

This Work (Liquid)	This Work (Micro-droplet)	Ref. [32] (Neat)	Ref. [33]	Ref. [33] (Theor.[a])	Approx. Description [33]
	231[b]				
372	363[b]	351	368	381	CH
384	387[b]				
	540[b]				
	568[b]				
	588[b]				
664	663	651	665	655	CC ring
	748[b]				
865	863	847	862		CC ring
1054	1054	1041	1054	1084	CC ring
1143	1127	1113	1127	1147	CH ring
1293	1291	1277	1287	1319	CC ring
1467	1465	1455	1465	1471	CH ring
1604	1601	1601	1617	1617	CC ring
1736	1734	1725	1739	1778	C = O
2760	2891		2912	2950	
2935	2934	2937	2948	2962	CH
2983	2981		2979	2985	CH
3080	3080	3078	3083	3077	CH ring

[a]Anharmonic vibrational frequencies calculated at the B3LYP/6-31G* level of theory [33].

[b]Peaks initially absent in the Raman spectrum of the bulk liquid.

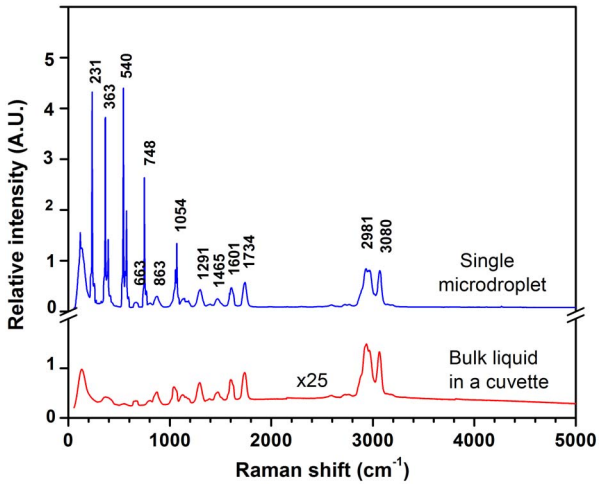

Fig. 2. Raman scattering spectra of diethyl phthalate from a single laser-trapped 21 μm microdroplet in the air (blue trace) or bulk liquid (red trace) in a cuvette. The recording integration time for each spectrum is 2 s.

dielectric microcavities (spheres, disks, rings) and the outer medium with a lower refractive index resulting from total internal reflection. The Raman signal can be enhanced by the input resonance when the illuminating wavelength matches a WGM, or by the output resonance when a Raman scattering wavelength matches a WGM. Double resonances contribute to very strong Raman sharp peaks, and have more opportunities to produce SRS and Raman laser emission, especially in a large microcavity with a high density of WGMs. Figure 3 shows the time evolution of Raman spectra from an optically trapped (a) DEPh and (b) glycerol microdroplet. Spectra were continuously recorded for about an hour at 1 min intervals as the particle size changed from about 20 μm to about 17 μm in diameter. During the particle shrinking period, both show their own clean consistent Raman scattering peaks in the more than 1 h recording time period, and some discrete sharp SRS peaks are observed for both materials all the time, especially strong in the 20–19 μm size range at the first 20 min spectral recording time.

Figure 4(a) presents one of these Raman scattering spectra shown in Fig. 3 from the single droplets of diethyl phthalate (black) and glycerol (red). Although the Raman spectra from

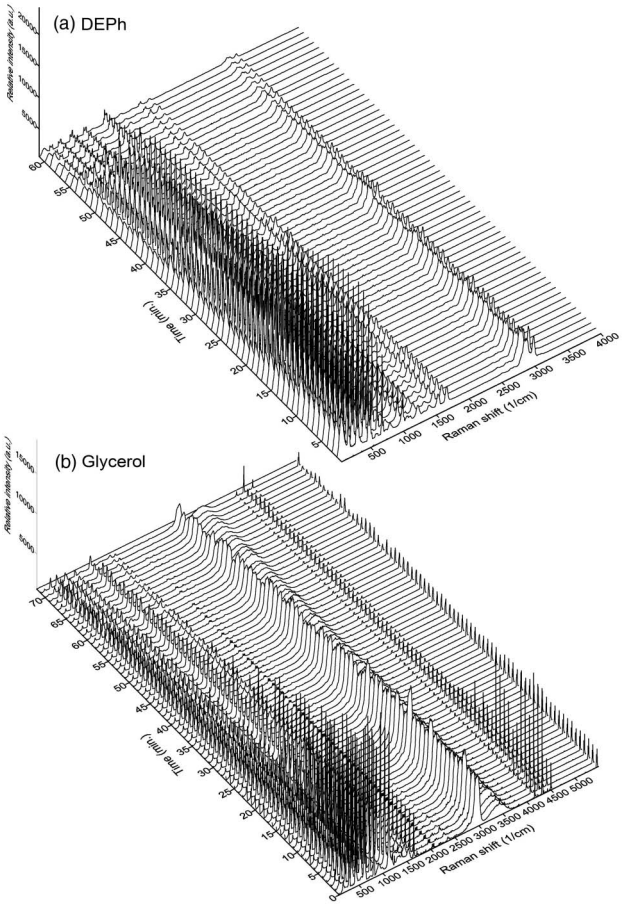

Fig. 3. Time evolution of the Raman spectrum of an optically trapped (a) DEPh and (b) glycerol microdroplet. Spectra were continuously recorded for about an hour at a 1 min interval with a 2 s integration time as the particle size changed from about 20 μm to about 17 μm in diameter.

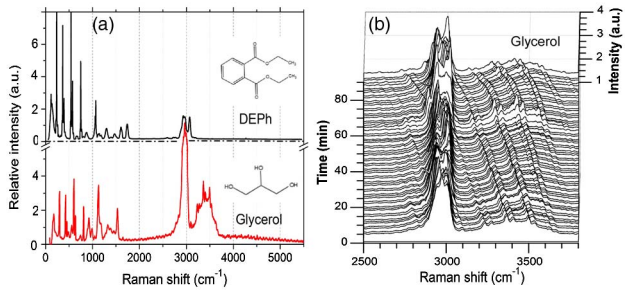

Fig. 4. (a) Typical Raman scattering spectra of a laser-trapped single diethyl phthalate (DEPh, black colored) and glycerol (red colored) microdroplet. (b) The observed WGMs over the O-H stretch vibrational band in a portion of the Raman spectrum of a laser-trapped microdroplet of glycerol. The plot depicts evaporation over a period of 120 min, where single scans were continuously taken at a 2 min interval. The WGM peaks over the O-H stretch mode shifted to the blue as the microdroplet size decreased during the evaporation process, while the spontaneous and stimulated Raman peak frequencies were unaffected during the particle size changing process.

the two chemicals demonstrate some peaks with similar shifts from the common C-H, C-C, and C-O bonds, they show a big distinguishable difference. It has been demonstrated that, as the microdroplet size changes, the Raman frequencies of these WGM resonance peaks are blueshifted during evaporation of the droplet and redshifted during growth of the droplet [16,46]. As glycerol has a broad O-H stretch band, it allows us to track the frequency shift of the WGM resonance peaks more easily than that from the sharp discrete spontaneous peaks. Figure 4(b) shows the time evolution of the Raman spectra of another laser-trapped glycerol microdroplet focusing at the O-H stretch band region. These spectra were continuously recorded for 120 min at a 2 min interval as the particle size changed from about 20 μm to about 14 μm in diameter. Noticeable WGM resonance frequencies of Raman peaks shifted to the blue as the microdroplet size decreased during the evaporation process, while the spontaneous peaks kept the same frequency, such as the broad C-H peak around 2950 cm^{-1}. This peak shape was slightly different from time to time, resulting from the superposition of WGM peaks. Although these resonance peaks in the droplet format give additional sharp features, they do not indicate any new molecular structures. They are microcavity-enhanced effected at the particular WGM resonance frequency based on the existing spontaneous scattering bands. As we know, all these process, such as the possibilities of contaminants from air, relative index changes due to the possible accumulation of the material as vapor near the droplet from the high hygroscopic nature of glycerol, or droplet deformation, will shift the resonance peaks. However, as the resonance WGM peaks in the O-H stretch band were continuously blueshifted, we consider they are mainly resulting from the shrink of the droplet that is dominated from the evaporation process during the observing period.

In parallel to the chemical composition characterization, we were able to determine the particle size of the trapped microdroplet by profiling the intensity of the elastic scattered light as a function of time. In our experiments, the scattered light was

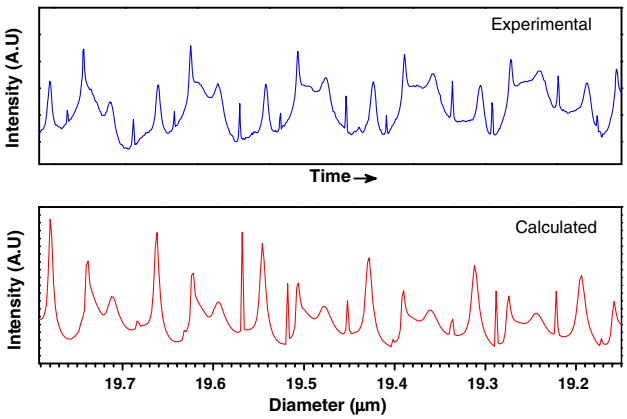

Fig. 5. Comparison between the experimental and calculated resonance spectra of the elastic scattering intensity at 90° from a laser-trapped diethyl phthalate microdroplet from 19.8 μm to 19.15 μm in diameter.

collected with an objective lens set at 90° with respect to the main axis of the incident beam and as predicted by the Lorenz–Mie theory [27,28]; the resulting spectrum (Fig. 5, upper panel) exhibits recurring sharp resonances peaks. The simulated spectrum (Fig. 5, lower panel) was computed at a 90° scattered angle for an unpolarized wave, using a refractive index of $m = 1.502$. The comparison between the experimental and theoretical results shows a good agreement with respect to the variation of the scattered light intensity during the evaporation of the droplet. However, it has been noted by Preston and Reid that the resonance spectrum might be significantly affected by spatial variation of a Bessel beam or other focused radiation beams from a plane wave illumination [47]. However, the small discrepancies in relative intensities (Fig. 5) do not prevent us from particle size determination by aligning related positions of the sharp resonance peaks. Not like determining particle size from elastic scattering intensity at one or a few angles at a time, this method recording the scattering intensity as a function of time can accurately assign the droplet to only one size.

4. CONCLUSION

We report a Raman spectrometer system for the detection and characterization of laser-trapped single chemical microdroplets. Diethyl phthalate and glycerol microdroplets were generated using a drop-on-demand single-jet dispersing device. A single microdroplet was efficiently trapped within a single-laser trapping system and spectroscopically interrogated using Raman scattering spectroscopy. The observed Raman shift frequencies are largely in excellent agreement with those from previous works and theoretical prediction. The uniqueness of the chemical fingerprint is enhanced by the appearance of additional spectral features related to the spherical nature of the microdroplets, namely stimulated Raman scattering and WGMs. We recorded the elastic scattered light intensity at a certain angle as a function of time, during evaporation of the droplet. The resulting resonance spectrum was compared to our simulation, based on Lorenz–Mie theory, to determine the microdroplet size at any given time. As intended, the proposed method was proven to be highly reproducible and stable, a single trapped microdroplet could be held for extended periods of time depending on its volatility (from a few minutes up to several hours for less volatiles compounds). Due to its high efficiency in trapping and its precision in spectroscopic characterization, this method could be particularly suitable for detecting and characterizing hazardous substances such as chemical agents in complex atmospheric environments.

Funding. Defense Threat Reduction Agency (DTRA) (HDTRA1621520); Army Research Laboratory (ARL) Mission funds.

Acknowledgment. The views and conclusions contained in this document are those of the authors and should not be interpreted as representing the official policies, either expressed or implied, of the Army Research Laboratory or the U.S. Government. The U.S. Government is authorized to reproduce and distribute reprints for Government purposes notwithstanding any copyright notation herein.

REFERENCES

1. OPCW, "Convention on the prohibition of the development, production, stockpiling and use of chemical weapons and on their destruction," (1993),https://www.opcw.org//.
2. K. K. Kroening, R. N. Easter, D. D. Richardson, S. A. Willison, and J. A. Caruso, *Analysis of Chemical Warfare Degradation Products* (Wiley, 2011).
3. A. B. Kanu, P. E. Haigh, and H. H. Hill, "Surface detection of chemical warfare agent simulants and degradation products," Anal. Chim. Acta **553**, 148–159 (2005).
4. V. Miller and M. Hogan, *Health Effects of Project Shad Chemical Agent: Diethylphthalate* (National Academies Silver Spring, 2004).
5. J. Lavoie, S. Srinivasan, and R. Nagarajan, "Using cheminformatics to find simulants for chemical warfare agents," J. Hazard. Mater. **194**, 85–91 (2011).
6. M. L. Good, "A proposed particle containment device," Technical Report UCRL-4146 (California University, 1953).
7. A. Ashkin, "Acceleration and trapping of particles by radiation pressure," Phys. Rev. Lett. **24**, 156–159 (1970).
8. A. Ashkin and J. M. Dziedzic, "Optical levitation by radiation pressure," Appl. Phys. Lett. **19**, 283–285 (1971).
9. R. N. Berglund and B. Y. H. Liu, "Generation of monodisperse aerosol standards," Environ. Sci. Technol. **7**, 147–153 (1973).
10. E. J. Davis, "A history of single particle levitation," Aerosol Sci. Technol. **26**, 212–254 (1997).
11. J. P. Reid and L. Mitchem, "Laser probing of single-aerosol droplet dynamics," Annu. Rev. Phys. Chem. **57**, 245–271 (2006).
12. K. Schaschek, J. Popp, and W. Kiefer, "Observation of morphology-dependent input and output resonances in time-dependent Raman spectra of optically levitated microdroplets," J. Raman Spectrosc. **24**, 69–75 (1993).
13. T. Kaiser, G. Roll, and G. Schweiger, "Investigation of coated droplets in an optical trap: Raman-scattering, elastic-light-scattering, and evaporation characteristics," Appl. Opt. **35**, 5918–5924 (1996).
14. M. D. King, K. C. Thompson, and A. D. Ward, "Laser tweezers Raman study of optically trapped aerosol droplets of seawater and oleic acid reacting with ozone: implications for cloud-droplet properties," J. Am. Chem. Soc. **126**, 16710–16711 (2004).
15. R. Symes, R. M. Sayer, and J. P. Reid, "Cavity enhanced droplet spectroscopy: principles, perspectives and prospects," Phys. Chem. Chem. Phys. **6**, 474–487. (2004).
16. L. Mitchem, J. Buajarern, R. J. Hopkins, A. D. Ward, R. J. Gilham, R. L. Johnston, and J. P. Reid, "Spectroscopy of growing and evaporat-

ing water droplets: exploring the variation in equilibrium droplet size with relative humidity," J. Phys. Chem. A **110**, 8116–8125 (2006).
17. J. R. Butler, L. Mitchem, K. L. Hanford, L. Treuel, and J. P. Reid, "*In situ* comparative measurements of the properties of aerosol droplets of different chemical composition," Faraday Discuss. **137**, 351–366; discussion 403-324 (2008).
18. M. Kriek, C. Neylon, P. L. Roach, I. P. Clark, and A. W. Parker, "A simple setup for the study of microvolume frozen samples using Raman spectroscopy," Rev. Sci. Instrum. **76**, 104301 (2005).
19. Y. L. Pan, S. C. Hill, and M. Coleman, "Photophoretic trapping of absorbing particles in air and measurement of their single-particle Raman spectra," Opt. Express **20**, 5325–5334 (2012).
20. C. Wang, Y. L. Pan, S. C. Hill, and B. Redding, "Photophoretic trapping-Raman spectroscopy for single pollens and fungal spores trapped in air," J. Quant. Spectrosc. Radiat. Transfer **153**, 4–12 (2015).
21. L. Ling and Y. Q. Li, "Measurement of Raman spectra of single airborne absorbing particles trapped by a single laser beam," Opt. Lett. **38**, 416–418 (2013).
22. R. L. Aggarwal, S. Di Cessa, L. W. Farrar, A. Shabshelowitz, and T. H. Jeys, "Sensitive detection and identification of isovanillin aerosol particles at a Pg/cm^3 mass concentration level using Raman spectroscopy," Aerosol Sci. Technol. **49**, 753–756 (2015).
23. B. Redding, S. C. Hill, D. Alexson, C. Wang, and Y. L. Pan, "Photophoretic trapping of airborne particles using ultraviolet illumination," Opt. Express **23**, 3630–3639 (2015).
24. A. Ashkin and J. M. Dziedzic, "Observation of radiation-pressure trapping of particles by alternating light beams," Phys. Rev. Lett. **54**, 1245–1248 (1985).
25. A. Ashkin and J. M. Dziedzic, "Optical levitation of liquid drops by radiation pressure," Science **187**, 1073–1075 (1975).
26. B. Redding and Y. L. Pan, "Optical trap for both transparent and absorbing particles in air using a single shaped laser beam," Opt. Lett. **40**, 2798–2801 (2015).
27. L. V. Lorenz, "Oeuvres scientifiques de L. Lorenz," in *Revues Et Annotées*, H. Valentiner, ed. (Librairie lehman & Stage, 1898).
28. W. Hergert and T. Wriedt, *The Mie Theory Basics and Applications*, Springer Series in Optical Sciences (Springer, 2012), Vol. **169**.
29. A. K. Ray, A. Souyri, E. J. Davis, and T. M. Allen, "Precision of light scattering techniques for measuring optical parameters of microspheres," Appl. Opt. **30**, 3974–3983 (1991).
30. V. V. Devarakonda and A. K. Ray, "Determination of thermodynamic parameters from evaporation of binary microdroplets of volatile constituents," J. Colloid Interface Sci. **221**, 104–113 (2000).
31. G. Gouesbet and G. Gréhan, *Generalized Lorenz-Mie Theories* (Springer, 2011).
32. R. L. Aggarwal, L. W. Farrar, B. G. Saar, T. H. Jeys, and R. B. Goodman, "Measurement of the absolute Raman cross sections of diethyl phthalate, dimethyl phthalate, ethyl cinnamate, propylene carbonate, tripropyl phosphate, 1, 3-cyclohexanedion, 3'-aminoacetaphenone, diethyl acetamidomalonate, isovanillin, lactide, meldrum's acid, P-tolyl sulfoxide and vanillin," Technical Report (Massachusetts Institute of Technology, 2013).
33. W. Meng, G. Jin-Ju, W. Zhong-Bo, and W. Zun-Yao, "FT-IR, Raman and NMR spectra, molecular geometry, vibrational assignments, Ab initio and density functional theory calculations for diethyl phthalate," Chin. J. Struct. Chem. **32**, 890–902 (2013).
34. R. Thurn and W. Kiefer, "Structural resonances observed in the Raman spectra of optically levitated liquid droplets," Appl. Opt. **24**, 1515–1519 (1985).
35. J. B. Snow, S. X. Qian, and R. K. Chang, "Stimulated Raman scattering from individual water and ethanol droplets at morphology-dependent resonances," Opt. Lett. **10**, 37–39 (1985).
36. V. E. Roman and J. Popp, "In situ microparticle diagnostic by stimulated Raman scattering," Phys. Chem. Chem. Phys. **1**, 5491–5495 (1999).
37. Y.-L. Pan, C. Wang, S. C. Hill, M. Coleman, L. A. Beresnev, and J. L. Santarpia, "Trapping of individual airborne absorbing particles using a counterflow nozzle and photophoretic trap for continuous sampling and analysis," Appl. Phys. Lett. **104**, 113507 (2014).
38. Z. Gong, Y. L. Pan, and C. Wang, "Optical configuration for photophoretic trap of single particles in air," Rev. Sci. Instrum. **87**, 103104 (2016).
39. K. C. Neuman and S. M. Block, "Optical trapping," Rev. Sci. Instrum. **75**, 2787–2809 (2004).
40. V. E. Roman, J. Popp, M. H. Fields, and W. Kiefer, "Minority species detection in aerosols by stimulated anti-stokes-Raman scattering and external seeding," Appl. Opt. **38**, 1418–1422 (1999).
41. L. Pasternack, J. W. Fleming, and J. C. Owrutsky, "Optically seeded stimulated Raman scattering of aqueous sulfate microdroplets," J. Opt. Soc. Am. B **13**, 1510–1516 (1996).
42. Y. H. Zhang, M. Y. Choi, and C. K. Chak, "Relating hygroscopic properties of magnesium nitrate to the formation of contact ion pairs," J. Phys. Chem. A **108**, 1712–1718 (2004).
43. A. Ashkin and J. M. Dziedzic, "Observation of optical resonances of dielectric spheres by light scattering," Appl. Opt. **20**, 1803–1814 (1981).
44. J. F. Owen, R. K. Chang, and P. W. Barber, "Morphology-dependent resonances in Raman scattering, fluorescence emission and elastic scattering from microparticles," Aerosol Sci. Technol. **1**, 293–302 (1982).
45. S. C. Hill, R. E. Benner, C. K. Rushforth, and P. R. Conwell, "Structural resonances observed in the fluorescence emission from small spheres on substrates," Appl. Opt. **23**, 1680–1683 (1984).
46. S. Anand, M. Eryurek, Y. Karadag, A. Erten, A. Serpenguzel, A. Jonas, and A. Kiraz, "Observation of whispering gallery modes in elastic light scattering from microdroplets optically trapped in a microfluidic channel," J. Opt. Soc. Am. B **33**, 1349–1354 (2016).
47. T. C. Preston and J. P. Reid, "Angular scattering of light by a homogeneous spherical particle in a zeroth-order Bessel beam and its relationship to plane wave scattering," J. Opt. Soc. Am. A **32**, 1053–1062 (2015).